

Research Article

Cite this article: Kant N, Singh A, Thakur V (2019). Second-harmonic generation by a chirped laser pulse with the exponential density ramp profile in the presence of a planar magnetostatic wiggler. *Laser and Particle Beams* **37**, 442–447. <https://doi.org/10.1017/S0263034619000739>

Received: 12 September 2019

Revised: 30 October 2019

Accepted: 6 November 2019



Key words:

Chirped laser pulse; exponential density ramp profile; magnetostatic wiggler; second-harmonic generation

Author for correspondence:

Vishal Thakur, Department of Physics, Lovely Professional University, G.T. Road, Phagwara 144411, Punjab, India.
E-mail: vishal20india@yahoo.co.in

Second-harmonic generation by a chirped laser pulse with the exponential density ramp profile in the presence of a planar magnetostatic wiggler

Niti Kant¹ , Arvinder Singh² and Vishal Thakur¹ 

¹Department of Physics, Lovely Professional University, G.T. Road, Phagwara 144411, Punjab, India and

²Department of Physics, NIT Jalandhar, Jalandhar 144 011, Punjab, India

Abstract

Second-harmonic generation of the relativistic self-focused chirped laser pulse in plasma has been studied with the exponential plasma density ramp profile in the presence of a planar magnetostatic wiggler. It is evident that the exponential plasma density ramp is helpful in enhancing second-harmonic generation as, with the introduction of the exponential plasma density ramp, self-focusing becomes stronger and hence, it leads to enhance the harmonic generation of the second order in the plasma. Also, it is observed that the efficiency of second-harmonic generation enhances significantly with an increase in the value of the chirp parameter. Further, the magnetostatic wiggler helps in enhancing the harmonic generation of the second order. This is due to the fact that dynamics of the oscillating electrons is altered due to the Lorentz force which, in turn, modifies the plasma wave and, hence, results in the efficient second-harmonic generation.

Introduction

The interaction of the high-power laser beams with plasma gives rise to a number of non-linear effects (Ganeev *et al.*, 2012). Some of these non-linear phenomena includes THz radiation generation (Kumar *et al.*, 2011; Vij *et al.*, 2019), wakefield acceleration (Ibbotson *et al.*, 2010), self-focusing (Aggarwal *et al.*, 2016; Kumar *et al.*, 2018; Thakur *et al.*, 2019), and harmonic generation (Tripathi *et al.*, 2009; Vij *et al.*, 2017; Sharma *et al.*, 2019). The phenomenon of harmonic generation is noteworthy in terms of laser–plasma interaction and has brought remarkable notice due to its various applications. Over the last few years, a great progress in the laser technology has been witnessed in which intensity of the laser beam has been amplified progressively. As the electric field of such lasers is relatively high and this forces electrons in the plasma channel to oscillate with the relativistic energy.

A Gaussian laser expels the electrons radially away from the central axis which is referred to as the electron cavitation. This charge displacement because of the expelled electrons removes ions and forms a channel having density depression on the axis. Hence, under the influence of ultra-intense Gaussian laser pulse, the plasma channel gets depleted from the region of high field to low field, which results in the establishment of the transverse density gradient. Sharma and Sharma (2012) investigated the second-harmonic generation in the presence of the static magnetic field with the extended paraxial ray approximation. They considered both the relativistic and ponderomotive non-linearity simultaneously and concluded that when a laser beam incident on the inhomogeneous magneto-plasma, a density gradient is created which is parallel to a static magnetic field. Further, the plasma wave at the pump wave frequency is caused which leads to the generation of second harmonic.

In most of the laser interactions with homogeneous plasma, it is observed that odd harmonics with laser frequency are produced (Mori *et al.*, 1993; Zeng *et al.*, 1996). However, in the presence of density gradient, second harmonics have been noticed. This is because of the laser-induced quiver motion of the electrons across the density gradient, which, in turn, gives rise to the perturbation in electron density. Density perturbation couples with quiver motion of electrons, which produces the source current at the second-harmonic frequency.

In this paper, for the first time, we point out the probability of the second-harmonic generation when the laser beam propagates in the homogeneous plasma under the influence of a planar magnetostatic wiggler with the exponential density profile. With the increase in the value of the positive chirp parameter, the second-harmonic generation enhances. Influence of cyclotron frequency associated with the plasma electrons is also seen in the enhancement of second-harmonic generation. It is due to the fact that dynamics of the oscillating electrons is altered due to the Lorentz force which, in turn, modifies the plasma wave and, hence, results in the efficient second-harmonic generation. As we know that the exponential plasma density

ramp is crucial for stronger self-focusing which further enhances the second-harmonic generation. In addition to this chirped pulse laser is considered as it increases the laser–plasma interaction for a longer duration. Also, wiggler magnetic field is introduced here, as it provides the necessary phase-matching condition. Therefore, the combined influence of exponential density ramp, wiggler magnetic field, and chirped pulse laser are considered here for an efficient second-harmonic generation. The construction of the manuscript is as follows: In the section “Theoretical considerations”, non-linear current density and the dispersion relations for the fundamental/pump and the second-harmonic frequencies have been observed. In the section “Second-harmonic generation”, the normalized wave amplitude of second harmonic and its conversion efficiency are derived. Numerical results and conclusions are given in the sections “Result and discussion” and “Conclusion”.

Theoretical considerations

Consider a linearly polarized chirped pulse laser propagating along the z direction under the influence of planar magnetostatic wiggler field \vec{B}_w . The wiggler field and vector potential of chirped pulse laser can be written as follows (Esmaildoost *et al.*, 2017):

$$\vec{B}_w = B_0(\hat{e}_y \sin(k_w z)), \tag{1}$$

$$\vec{A} = \hat{e}_x A(z, t) \sin(k_1 z - \omega_1 t), \tag{2}$$

where B_0 is the amplitude of the magnetic field, $k_w = 2\pi/\lambda_w$ represents the wave number of the wiggler field, $\omega_1 = \omega_0(1 + b(\omega_0 t - \omega_0 z/c))$ is the frequency of chirped pulse laser, b represents the chirp parameter, c represents the velocity of the light in the vacuum, ω_0 is the laser frequency, $k_1 = \omega_0(1 + b(\omega_0 t - \omega_0 z/c))\mu_1/c$ is the propagation vectors at frequencies ω_0 , and μ_1 is the refractive index for fundamental wave. Further, following Jha *et al.* (2007), penetration of laser beam through the transversely magnetized plasma generates transverse current density at the frequency $2\omega_0$ and acts as the source for the generation of second harmonic. As a result, for frequencies ω_0 and $2\omega_0$, the vector potential can be given as follows:

$$\vec{A}_1 = \hat{e}_x A_1 \sin(k_1 z - \omega_1 t), \tag{3}$$

$$\vec{A}_2 = \hat{e}_x A_2 \sin(k_2 z - 2\omega_1 t), \tag{4}$$

where A_1 and A_2 are amplitudes of the laser beam and its second harmonic, respectively, $k_2 = 2\omega_0(1 + b(\omega_0 t - \omega_0 z/c))\mu_2/c$ is the propagation vector at the frequency $2\omega_0$, and μ_2 is the refractive index for the second-harmonic wave.

Further, using Maxwell’s equations, we obtain the wave equation as follows:

$$\left(-\nabla^2 + \frac{1}{c^2} \frac{\partial^2}{\partial t^2}\right) A = \frac{4\pi}{c} J, \tag{5}$$

$$J = -n_e e v_e, \tag{6}$$

where J is the current density of plasma electrons, n_e is the electron density, e is the magnitude of electron charge, and v_e represents the electron velocity.

Also, the relativistic equation of motion for the electrons is written as follows:

$$\frac{\partial(\gamma m_{0e} v_e)}{\partial t} = -e \left[E + \frac{1}{c} v_e \times B_w \right] - \frac{1}{n_e} \nabla p_e, \tag{7}$$

and the continuity equation is

$$\frac{\partial n}{\partial t} + \vec{\nabla} \cdot (n_e \vec{v}_e) = 0, \tag{8}$$

where p_e represents the pressure of electrons, and m_{0e} is electron’s rest mass. Further, the continuity equation is $\partial n/\partial t + \vec{\nabla} \cdot (n_e \vec{v}_e) = 0$, where $\gamma = \sqrt{1 + p_e^2/m_{0e}^2 c^2}$ is the relativistic factor. By substituting Eq. (1) into Eq. (7), velocity in x- and z-directions are given by $\partial v_x^{(1)}/\partial t = -e E_1/m_{0e} + v_z^{(1)} \omega_w \sin(k_w z)$ and $\partial v_z^{(1)}/\partial t = -e E_z^{(1)}/m_{0e} - v_x^{(1)} \omega_w \sin(k_w z)$, respectively, where $E_z^{(1)}$, $E_1 = -\partial A_1/\partial t$, $\omega_w = eB_0/m_{0e}c$ are first-order perturbation for the polarization field, the amplitude of the laser field, and the wiggler frequency, respectively. Further, first-order transverse and longitudinal velocities can be given as follows:

$$v_x^{(1)} = \frac{ca_1(\omega_0^2 - \omega_p^2)}{(\omega_0^2 - \omega_p^2 - \omega_w^2 \sin^2(k_w z))} \times \sin(k_w z) \cos(k_1 z - \omega_0(1 + b(\omega_0 t - \omega_0 z/c))t), \tag{9}$$

$$v_z^{(1)} = -\frac{ca_1 \omega_w \omega_0}{(\omega_0^2 - \omega_p^2 - \omega_w^2 \sin^2(k_w z))} \times \sin(k_w z) \cos(k_1 z - \omega_0(1 + b(\omega_0 t - \omega_0 z/c))t), \tag{10}$$

where $a_1 = eA_1/mc\omega_0$ is the normalized amplitude of the pump wave, $\omega_p = (4\pi n(z')e^2/m_{0e})^{1/2}$ represents plasma frequency, $\omega_{p0} = 4\pi n_0 e^2/m_{0e}$, $z' = \omega_0 z/c$ is the normalized distance of propagation, $k'_w = k_w c/\omega$ is the normalized wiggler wave number. The plasma density profile is considered as $n(z') = n_0 \exp(z'/d)$, where d is the adjustable constant, n_0 is the equilibrium electron density, and e is the charge of the electron.

$$J_x^{(1)}(\omega_0) = \frac{a_1 n_0 (\omega_0^2 - \omega_{p0}^2 \exp(z'/d))}{(\omega_0^2 - \omega_{p0}^2 \exp(z'/d) - \omega_w^2 \sin^2(k'_w z'))} \times \sin(k'_w z') \sin(k_1 z - \omega_0(1 + b(\omega_0 t - z'))t). \tag{11}$$

By using Eqs (5) and (11), non-linear dispersion relation can be obtained as follows:

$$c^2 k_1^2 = \omega_0^2 - \frac{(\omega_0^2 - \omega_{p0}^2 \exp(z'/d)) \omega_{p0}^2 \exp(z'/d)}{(\omega_0^2 - \omega_{p0}^2 \exp(z'/d) - \omega_w^2 \sin^2(k'_w z'))}. \tag{12}$$

Further, in the absence of the wiggler field, Eq. (12) reduces to dispersion relation in the linear limit. The refractive index

associated with the frequency ω_0 can be written as follows:

$$n_1 = \left(1 - \frac{(\omega_0^2 - \omega_{p0}^2 \exp(z'/d))\omega_{p0}^2 \exp(z'/d)}{\omega_0^2(\omega_0^2 - \omega_{p0}^2 \exp(z'/d) - \omega_w^2 \sin^2(k'_w z'))} \right)^{1/2} \quad (13)$$

Similarly, for the frequency $2\omega_0$, we have

$$n_2 = \left(1 - \frac{(\omega_0^2 - \omega_{p0}^2 \exp(z'/d))\omega_{p0}^2 \exp(z'/d)}{4\omega_0^2(4\omega_0^2 - \omega_{p0}^2 \exp(z'/d) - \omega_w^2 \sin^2(k'_w z'))} \right)^{1/2} \quad (14)$$

By employing perturbation theory and Eq. (8), we can derive the first-order plasma electron density as follows:

$$n^{(1)} = \frac{a_1 c n_0 k_1 \omega_w \sin(k'_w z') \cos(k_1 z - \omega_0(1 + b(\omega_0 t - z'))t)}{(\omega_0^2 - \omega_{p0}^2 \exp(z'/d) - \omega_w^2 \sin^2(k'_w z'))} \quad (15)$$

In a similar way, the second-order velocity component can be given as follows:

$$v_x^{(2)} = \frac{c^2 a_1^2 k_1 \omega_w [(\omega_0^2 - \omega_p^2)^2 - (\omega_w^2 \sin^2(k_w z))((4\omega_0^2 - \omega_p^2))]}{2(\omega_0^2 - \omega_p^2 - \omega_w^2 \sin^2(k_w z))(4\omega_0^2 - \omega_p^2 - \omega_w^2 \sin^2(k_w z))} \times \sin(k_w z) \sin 2(k_1 z - \omega_0(1 + b(\omega_0 t - \omega_0 z/c))t) \quad (16)$$

Following the same steps to calculate the first order $n^{(1)}$, the second-order plasma electron density can be given as follows:

$$n^{(2)} = \left[\frac{a_1^2 c^2 n_0 k_1^2 [(\omega_0^2 - \omega_{p0}^2 \exp(z'/d))^2 - \omega_w^2 \sin^2(k'_w z')(4\omega_0^2 - \omega_{p0}^2 \exp(z'/d))]}{(\omega_0^2 - \omega_{p0}^2 \exp(z'/d) - \omega_w^2 \sin^2(k'_w z'))^2 (4\omega_0^2 - \omega_{p0}^2 \exp(z'/d) - \omega_w^2 \sin^2(k'_w z'))} \right] \times \cos 2(k_1 z - \omega_0(1 + b(\omega_0 t - z'))) \quad (17)$$

As we know harmonics are driven by the non-linear current density; hence, we can derive second-order equations of the non-linear current density for second harmonic by using $J_x^{(2)} = -e(n_0 v_x^{(2)} + n^{(1)} v_x^{(1)})$ and Eq. (16). As a result, one can have

$$J_x^{(2)}(2\omega_0) = \left[\frac{3a_1^2 c^2 e n_0 k_1 \omega_w \omega_0^2 (\omega_0^2 - \omega_{p0}^2 \exp(z'/d) + \omega_w^2 \sin^2(k'_w z'))}{2(\omega_0^2 - \omega_{p0}^2 \exp(z'/d) - \omega_w^2 \sin^2(k'_w z')) \times (4\omega_0^2 - \omega_{p0}^2 \exp(z'/d) - \omega_w^2 \sin^2(k'_w z'))} \right] \times \sin(k'_w z') \sin 2(k_1 z - \omega_0(1 + b(\omega_0 t - z'))t) \quad (18)$$

Second-harmonic generation

By using Eqs (5) and (18), one can derive the expression for the amplitude of the second-harmonic field. We are considering that distance over which $\partial a_2(z)/\partial z$ changes considerably is large as compared with the wavelength ($\partial^2 a_2(z)/\partial z^2 \ll k_2 \partial a_2(z)/\partial z$) and that A_1 reduces very slightly. Here, $a_2(z)$ represents the normalized amplitude of the second-harmonic wave. The quantity a_1^2 can be assumed to be independent of z and growth of the second harmonic is given as follows:

$$a_2(z) = \frac{3a_1^2 \omega_w \sin(k'_w z') \omega_{p0}^2 \exp(z'/d) \left[1 - \frac{\omega_{p0}^2 \exp(z'/d)}{\omega_0^2(1 + b(\omega_0 t - z'))^2} \left(1 - \frac{\omega_{p0}^2 \exp(z'/d)}{\omega_0^2(1 + b(\omega_0 t - z'))^2} \right) \right]^{1/2} \times \left(1 - \frac{\omega_{p0}^2 \exp(z'/d)}{\omega_0^2(1 + b(\omega_0 t - z'))^2} + \frac{\omega_w^2 \sin^2(k'_w z')}{\omega_0^2(1 + b(\omega_0 t - z'))^2} \right) \exp \left[\frac{i\Delta k z}{2} \right] \frac{\sin \left(\frac{\Delta k z}{2} \right)}{\Delta k}}{16c\omega_0^2 \left[1 - \frac{\omega_{p0}^2 \exp(z'/d)}{4\omega_0^2(1 + b(\omega_0 t - z'))^2} \left(1 - \frac{\omega_{p0}^2 \exp(z'/d)}{4\omega_0^2(1 + b(\omega_0 t - z'))^2} \right) \right]^{1/2} \times \left(1 - \frac{\omega_{p0}^2 \exp(z'/d)}{4\omega_0^2(1 + b(\omega_0 t - z'))^2} - \frac{\omega_w^2 \sin^2(k'_w z')}{4\omega_0^2(1 + b(\omega_0 t - z'))^2} \right) \times \left(1 - \frac{\omega_{p0}^2 \exp(z'/d)}{4\omega_0^2(1 + b(\omega_0 t - z'))^2} - \frac{\omega_w^2 \sin^2(k'_w z')}{4\omega_0^2(1 + b(\omega_0 t - z'))^2} \right)} \quad (19)$$

where $\Delta k = 2k_1 - k_2$. Further, the second-harmonic conversion efficiency $\eta_2(z)$ can be given as follows:

By using Eqs (19) and (20), we obtain the following equation:

$$\eta_2(z) = \frac{n_1}{n_2} \frac{\left| \frac{\partial a_2}{\partial t} \right|^2}{\left| \frac{\partial a_1}{\partial t} \right|^2}. \tag{20}$$

$$\eta_2(z) = \frac{9a_1^2 \omega_w^2 \sin^2(k'_w z') \omega_{p0}^4 \exp(z'/d) \left[1 - \frac{\frac{\omega_{p0}^2 \exp(z'/d)}{\omega_0^2(1+b(\omega_0 t - z'))^2} \left(1 - \frac{\omega_{p0}^2 \exp(z'/d)}{\omega_0^2(1+b(\omega_0 t - z'))^2} \right)}{\left(1 - \frac{\omega_{p0}^2 \exp(z'/d)}{\omega_0^2(1+b(\omega_0 t - z'))^2} - \frac{\omega_w^2 \sin^2(k'_w z')}{\omega_0^2(1+b(\omega_0 t - z'))^2} \right)} \right]^{1/2} \times \left(1 - \frac{\omega_{p0}^2 \exp(z'/d)}{\omega_0^2(1+b(\omega_0 t - z'))^2} + \frac{\omega_w^2 \sin^2(k'_w z')}{\omega_0^2(1+b(\omega_0 t - z'))^2} \right) \left(\frac{\sin\left(\frac{\Delta k z}{2}\right)}{\Delta k} \right)^2}{128c^2 \omega_0^4 \left[1 - \frac{\frac{\omega_{p0}^2 \exp(z'/d)}{4\omega_0^2(1+b(\omega_0 t - z'))^2} \left(1 - \frac{\omega_{p0}^2 \exp(z'/d)}{4\omega_0^2(1+b(\omega_0 t - z'))^2} \right)}{\left(1 - \frac{\omega_{p0}^2 \exp(z'/d)}{4\omega_0^2(1+b(\omega_0 t - z'))^2} - \frac{\omega_w^2 \sin^2(k'_w z')}{4\omega_0^2(1+b(\omega_0 t - z'))^2} \right)} \right]^{1/2} \times \left(1 - \frac{\omega_{p0}^2 \exp(z'/d)}{\omega_0^2(1+b(\omega_0 t - z'))^2} - \frac{\omega_w^2 \sin^2(k'_w z')}{\omega_0^2(1+b(\omega_0 t - z'))^2} \right)^4 \times \left(1 - \frac{\omega_{p0}^2 \exp(z'/d)}{4\omega_0^2(1+b(\omega_0 t - z'))^2} - \frac{\omega_w^2 \sin^2(k'_w z')}{4\omega_0^2(1+b(\omega_0 t - z'))^2} \right)^2}. \tag{21}$$

The minimum value of the z for which the value of η is found to be maximum can be given as follows:

$$z = l_c = \frac{\pi}{\Delta k}, \tag{22}$$

where l_c represents the plasma length. Further, the maximum second harmonic efficiency is written as follows:

$$\eta_{\max} = \frac{9a_1^2 \omega_w^2 \sin^2(k'_w z') \omega_{p0}^4 \exp(z'/d) \left[1 - \frac{\frac{\omega_{p0}^2 \exp(z'/d)}{\omega_0^2(1+b(\omega_0 t - z'))^2} \left(1 - \frac{\omega_{p0}^2 \exp(z'/d)}{\omega_0^2(1+b(\omega_0 t - z'))^2} \right)}{\left(1 - \frac{\omega_{p0}^2 \exp(z'/d)}{\omega_0^2(1+b(\omega_0 t - z'))^2} - \frac{\omega_w^2 \sin^2(k'_w z')}{\omega_0^2(1+b(\omega_0 t - z'))^2} \right)} \right]^{1/2} \times \left(1 - \frac{\omega_{p0}^2 \exp(z'/d)}{\omega_0^2(1+b(\omega_0 t - z'))^2} + \frac{\omega_w^2 \sin^2(k'_w z')}{\omega_0^2(1+b(\omega_0 t - z'))^2} \right) \left(\frac{1}{\Delta k} \right)^2}{128c^2 \omega_0^4 \left[1 - \frac{\frac{\omega_{p0}^2 \exp(z'/d)}{4\omega_0^2(1+b(\omega_0 t - z'))^2} \left(1 - \frac{\omega_{p0}^2 \exp(z'/d)}{4\omega_0^2(1+b(\omega_0 t - z'))^2} \right)}{\left(1 - \frac{\omega_{p0}^2 \exp(z'/d)}{4\omega_0^2(1+b(\omega_0 t - z'))^2} - \frac{\omega_w^2 \sin^2(k'_w z')}{4\omega_0^2(1+b(\omega_0 t - z'))^2} \right)} \right]^{1/2} \times \left(1 - \frac{\omega_{p0}^2 \exp(z'/d)}{\omega_0^2(1+b(\omega_0 t - z'))^2} - \frac{\omega_w^2 \sin^2(k'_w z')}{\omega_0^2(1+b(\omega_0 t - z'))^2} \right)^4 \times \left(1 - \frac{\omega_{p0}^2 \exp(z'/d)}{4\omega_0^2(1+b(\omega_0 t - z'))^2} - \frac{\omega_w^2 \sin^2(k'_w z')}{4\omega_0^2(1+b(\omega_0 t - z'))^2} \right)^2}. \tag{23}$$

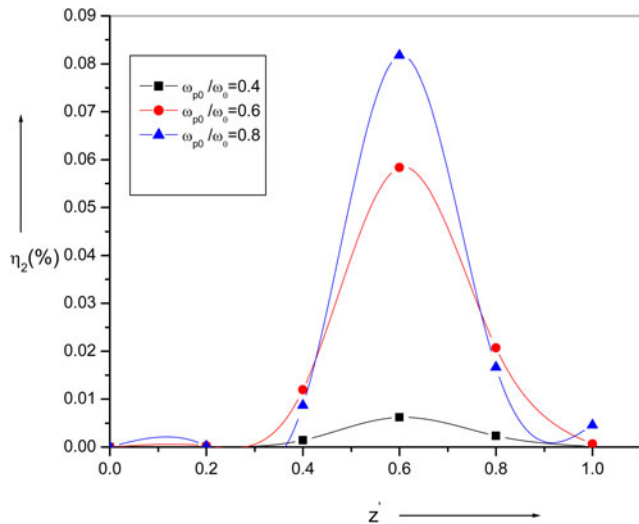


Fig. 1. Dependence of the conversion efficiency (η_2) on the normalized propagation distance z' for different values of ω_{p0}/ω_0 . Other parameters are $d = 10$, $b = 0.7$, and $\omega_w/\omega_0 = 0.06$.

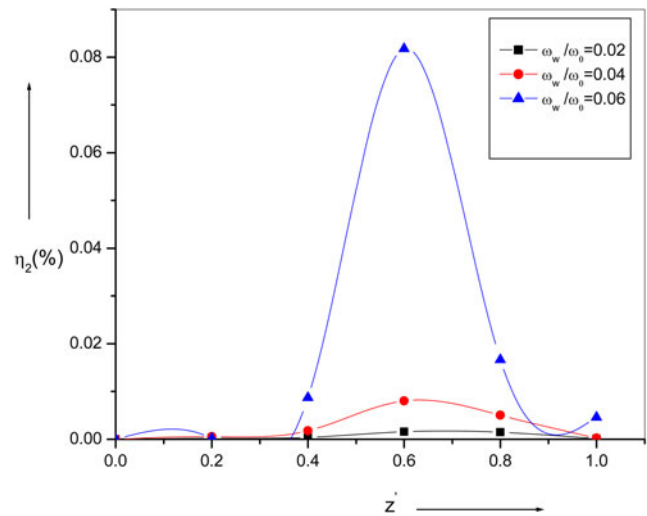


Fig. 2. Dependence of the conversion efficiency (η_2) on the normalized propagation distance z' for different values of ω_w/ω_0 . Rest of the parameters are same as taken in Figure 1.

Result and discussion

In order to obtain conversion efficiency of the second-harmonic generation, Eq. (21) is solved numerically. Consider plasma irradiated by a 1.06 μm Nd:YAG laser (intensity $I_0 \approx 5 \times 10^{17} \text{ W/cm}^2$). Figure 1 depicts the dependence of conversion efficiency (η) upon the normalized distance of propagation z' for different values of $\omega_{p0}/\omega_0 = 0.4, 0.6$, and 0.8 (corresponding electron density values are 1.58×10^{19} , 3.01×10^{19} , and $6.05 \times 10^{19} \text{ cm}^{-3}$, respectively). Rest of the values are $d = 10$, $b = 0.7$, and $\omega_w/\omega_0 = 0.06$. The maximum value of η is found to be 0.08% for $\omega_{p0}/\omega_0 = 0.8$ at normalized distance $z' = 0.6$. It is because, with the density of the plasma channel, the second-harmonic generation shows an oscillatory behavior and peaks at certain plasma density. Lorentz force influences the dynamics of oscillating electrons which, in turn, alters the plasma wave. This, in turn, enhances the second harmonic significantly. Further, it is observed that cyclotron frequency related to the plasma electrons in the presence of the exponential density ramp plays a key role in the enhancement of the harmonic generation of the second order. Similar effects were obtained previously in our work (Thakur *et al.*, 2018) and reported that the conversion efficiency of second-harmonic generation depends on the laser and plasma frequencies.

Figure 2 shows the variation of the conversion efficiency (η) with z' for different values of $\omega_w/\omega_0 = 0.02, 0.04$, and 0.06 . Rest of the parameters are same as detailed in Figure 1. It is studied that with an increase in the transverse magnetic field efficiency of the second-harmonic generation enhances considerably. Cyclotron frequency related to plasma electrons under exponential density transition plays a key role in enhancement of the harmonic generation of the second order. Figure 3 shows the conversion efficiency (η) for the various values of the chirped parameter $b = 0.3, 0.5$, and 0.7 . Rest of parameters are same as taken in Figure 1. The sharp rise in the conversion efficiency ($\approx 0.08\%$) of the second-harmonic amplitude is noticed for $b = 0.7$. This is because of the efficient electron heating

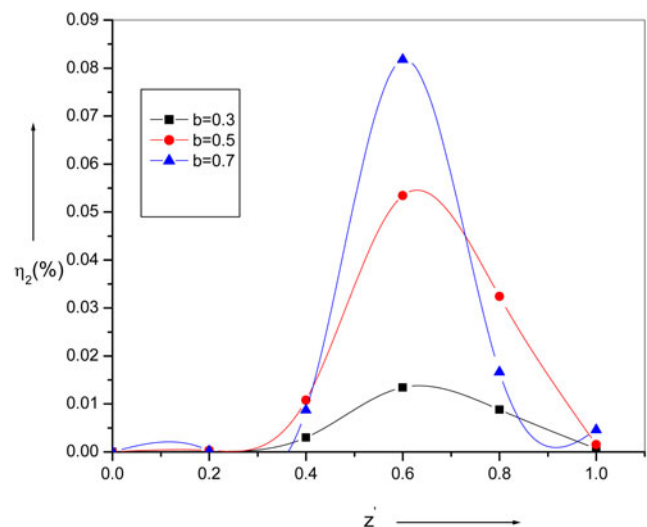


Fig. 3. Dependence of the conversion efficiency (η_2) on the normalized propagation distance z' for different values of the chirped parameter b . Rest of the parameters are same as taken in Figure 1.

by the shorter wavelength component of the chirped pulses which results in higher second-order susceptibility. The results are in good agreement with Jha *et al.* (2009). Equations describing the evolution of the phase shift and laser spot size were derived to analyze the propagation of the chirped laser pulses in a plasma channel. The enhancement in the conversion efficiency is observed with an increase in the chirp parameter value for positive chirp as shown in Figure 3. The physics behind this is that chirped laser pulse either positive or negative causes in the heating of the electrons which results in the enhancement of the second-harmonic generation as studied by Guo *et al.* (2001). Further, the influence of the exponential plasma density ramp is observed in making the self-focusing of the laser beam efficient which, in turn, enhances the second-harmonic generation.

Conclusion

In present work, we investigate the second-harmonic generation of the relativistic self-focusing chirped pulse laser under the influence of the exponential density transition with a planar magnetostatic wiggler. It is observed that conversion efficiency for the second harmonic increases as the wave progresses along the z direction under the exponential density transition. Under the influence of exponential density transition, fundamental laser beam propagates up to larger distance without getting so much divergence, and hence, plasma density ramp plays a major role in enhancing self-focusing. Also, with the increase in the chirp parameter value in the positive direction, the enhancement in the second-harmonic generation is observed. Further, the magnetostatic wiggler helps in enhancing the harmonic generation of the second order. This is due to the fact that dynamics of the oscillating electrons is changed due to the Lorentz force which, in turn, modifies the plasma wave and, hence, results in the efficient second-harmonic generation.

Financial support. This work is supported by the TARE Scheme (Grant No. TAR/2018/000916) of SERB, DST, New Delhi, India.

References

- Aggarwal M, Kumar H and Kant N (2016) Propagation of Gaussian laser beam through magnetized cold plasma with increasing density ramp. *Optik* **127**, 2212–2216.
- Esmacidoost N, Zolghadr S and Jafari S (2017) Self-focusing property of a laser beam interacting with a lattice of nanoparticles in the presence of a planar magnetostatic wiggler. *Journal of Applied Physics* **121**, 113106.
- Ganev RA, Hutchison C, Witting T, Frank F, Okell WA, Zair A, Weber S, Redkin PV, Lei DY, Roschuk T, Maier SA, L'Opez-Quintas I, Martin M, Castillejo M, Tisch JWG and Marangos JP (2012) High-order harmonic generation in graphite plasma plumes using ultrashort laser pulses: a systematic analysis of harmonic radiation and plasma conditions. *Journal of Physics B: Atomic, Molecular and Optical Physics* **45**, 165402.
- Guo C, Rodriguez G and Taylor AJ (2001) Propagation of chirped laser pulses in a plasma channel. *Physical Review Letters* **86**, 1638.
- Ibbotson TPA, Bourgeois N, Rowlands-Rees TP, Caballero LS, Bajlekov SI, Walker PA, Kneip S, Mangles SPD, Nagel SR, Palmer CAJ, DeLerue N, Doucas G, Urner D, Chekhlov O, Clarke RJ, Divall E, Ertel K, Foster PS, Hawkes SJ, Hooker CJ, Parry B, Rajeev PP, Streeter MJV and Hooker SM (2010) Laser-wakefield acceleration of electron beams in a low density plasma channel. *Physical Review Special Topics – Accelerators and Beams* **13**, 031301.
- Jha P, Mishra RK, Raj G and Upadhyay AK (2007) Second harmonic generation in laser magnetized-plasma interaction. *Physics of Plasmas* **14**, 053107.
- Jha P, Malviya A and Upadhyay AK (2009) Propagation of chirped laser pulses in a plasma channel. *Physics of Plasmas* **16**, 063106.
- Kumar G, Pandey S, Cui A and Nahata A (2011) Planar plasmonic terahertz waveguides based on periodically corrugated metal films. *New Journal of Physics* **13**, 033024.
- Kumar H, Aggarwal M, Richa and Gill TS (2018) Self-focusing of an elliptic-Gaussian laser beam in relativistic ponderomotive plasma using a ramp density profile. *Journal of the Optical Society of America B* **35**, 2212–2216.
- Mori WB, Decker CD and Leemans WP (1993) Relativistic harmonic content of nonlinear electromagnetic waves in underdense plasmas. *IEEE Transactions on Plasma Science* **21**, 110.
- Sharma P and Sharma RP (2012) Study of second harmonic generation by high power laser beam in magneto plasma. *Physics of Plasmas* **19**, 122106.
- Sharma V, Thakur V and Kant N (2019) Third harmonic generation of a relativistic self-focusing laser in plasma in the presence of wiggler magnetic field. *High Energy Density Physics* **32**, 51–55.
- Thakur V, Vij S, Sharma V and Kant N (2018) Influence of exponential density ramp on second harmonic generation by a short pulse laser in magnetized plasma. *Optik* **171**, 523–528.
- Thakur V, Wani MA and Kant N (2019) Relativistic self-focusing of Hermite-cosine-Gaussian laser beam in collisionless plasma with exponential density transition. *Communications in Theoretical Physics* **71**, 736–740.
- Tripathi VK, Liu CS, Shao X, Eliasson B and Sagdeev RZ (2009) Laser acceleration of monoenergetic protons in a self-organized double layer from thin foil. *Plasma Physics and Controlled Fusion* **51**, 024014.
- Vij S, Aggarwal M and Kant N (2017) Phase-matched relativistic second harmonic generation in clusters with density ripple. *Optics Communications* **383**, 349–354.
- Vij S, Kant N and Thakur V (2019) Resonant enhancement of terahertz radiation through vertically aligned carbon nanotubes array by applying wiggler magnetic field. *Plasmonics* **14**, 1051–1056.
- Zeng G, Shen B, Yu W and Xu Z (1996) Relativistic harmonic generation excited in the ultrashort laser pulse regime. *Physics of Plasmas* **3**, 4220.